Stress and Deflection Analysis in Distal Tibia Implant Plates

Adrian Tabula, Guangyang Cai, Wei Zhuo and Bochao Lu
Department of Bioengineering, University of California, Berkeley

Abstract:
Finite element analysis (FEA) has proven to be a valuable technique in studying bone fractures and implant plates to treat fractures. However, there has been relatively little usage of FEA to study distal tibia fractures. There is also little use of FEA to provide mechanical explanations for observations from clinical research about implant complications such as patient pain and bone density loss. To address these issues, our group used analytical modeling and FEA through COMSOL modeling to study the distal tibia attached to a locking implant plate. COMSOL modeling revealed high stress concentrations around the first and second top screws of the implant plate and an uneven distribution of stress in the tibia bone supported by the implant. These results from FEA could potentially be utilized to interpret clinical observations and predict potential implant complications.

Introduction:
A common method used to treat long bone fractures is the implantation of locking plates, which support and stabilize the fractured bone under both axial and torsional loading conditions. Research into bone fractures and locking plates has utilized finite element analysis to investigate the interactions of the plate and the bone. For instance, an article by Latifi et al. used finite element analysis (FEA) to demonstrate the efficiency of a locking plate in stabilizing a subtrochanteric fracture in the femur (9). Furthermore, FEA has been used by researchers to investigate the effectiveness of locking plates in healing tibia fractures and the formation of calluses on the bone due to implant-bone contact (8).

However, during our review of the research literature, we noticed two issues. First, there seems to be little research done on locking plates and distal tibia fractures, which are fractures that occur in the lower half of the tibia. The distal tibia is an important bone region to study as forces experienced within this region can be as high as 4.7 times a person's body weight (5). Also, there seems to be little use of FEA in predicting potential long-term effects of implant plates on bone after the fracture has healed. Clinical research has shown that excessively strong implants weaken the surrounding bone and lower bone mineral density (1). Also, patients will sometimes have tibia locking plates removed due to feeling constant pain from the implant (3). FEA could provide important insights into the mechanical reasons behind these long-term complications.

In order to address these key issues, we set two objectives we wanted to accomplish. (i) First, we wanted to model part of a distal tibia locking plate to see whether a stress comparison between the bone and the implant could provide a mechanical explanation for patient complaints about implant pain and bone weakening surrounding biomedical implants. (ii) Second, we wanted to see if deflection of the implant due to torque from the nails had any significant role in behind patient complaints about pain. To achieve these goals, we created a simplified analytical model for the distal tibia connected to a locking plate. We then compared our calculations from this analytical model to our results from COMSOL modeling.

Results:
From our analytical model, we calculated the maximum stress in the implant to be 2.284×10^7 Pa and the deflection as -2.446×10^{-4} m. From our COMSOL model, we saw a maximum downward normal stress of 4.791×10^7 Pa located at the first screw position (Fig. 1A) and a displacement of roughly -1.7×10^{-4} m for the implant region between the first and second screw (Fig. 2). From the overall model, we saw that stress was concentrated at the first screw position and rapidly decreased after the second screw (Fig. 1B and 1A). Stress is then evenly distributed in the implant after the second screw position at around -1.1×10^7 Pa. From Fig. 3B between the first and second screw positions, we see that the bone region closest to the implant experiences a reduced stress of -0.5×10^7 Pa compared to the -0.9×10^7 Pa experienced by the region of bone farthest away from the implant (Fig. 3B). A cross-sectional slice of the top of the bone unsupported by the implant reveals a stress of roughly -0.8×10^7 Pa (Fig. 3A).

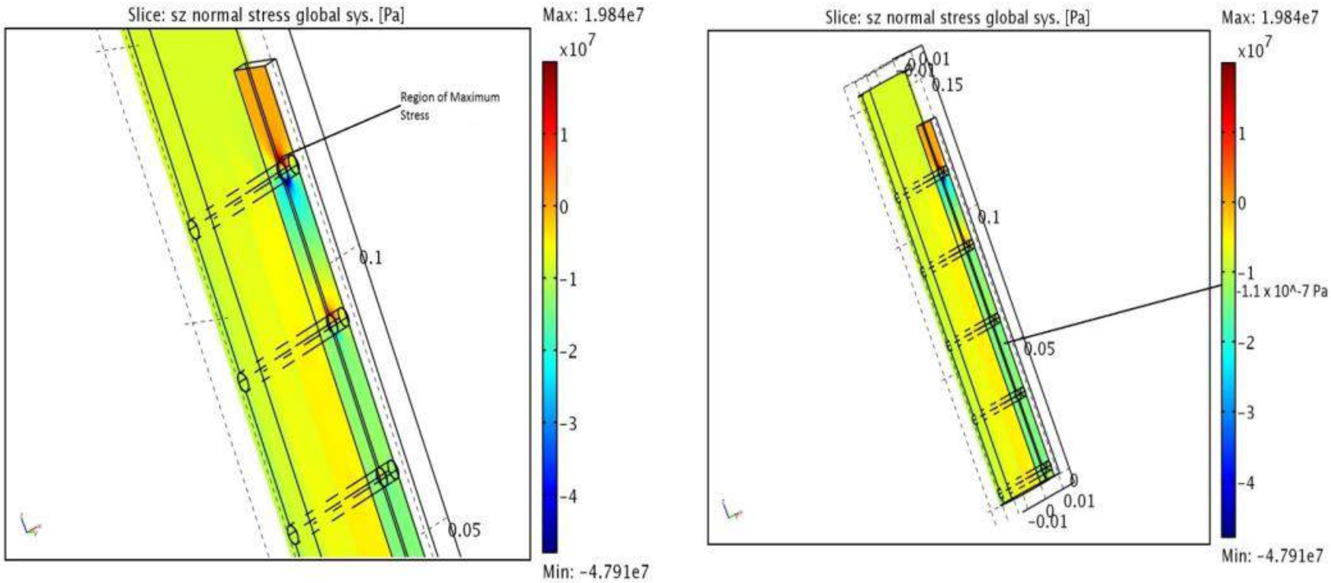

A) **B)**

Figure 1 Normal stress distribution generated from COMSOL. A). Maximum downward normal stress of 4.791 x 10^7 Pa located at the first screw position. The stress was concentrated at the first screw position and rapidly decreased after the second screw. B) Stress is then evenly distributed in the implant after the second screw position at around -1.1 x 10^7 Pa.

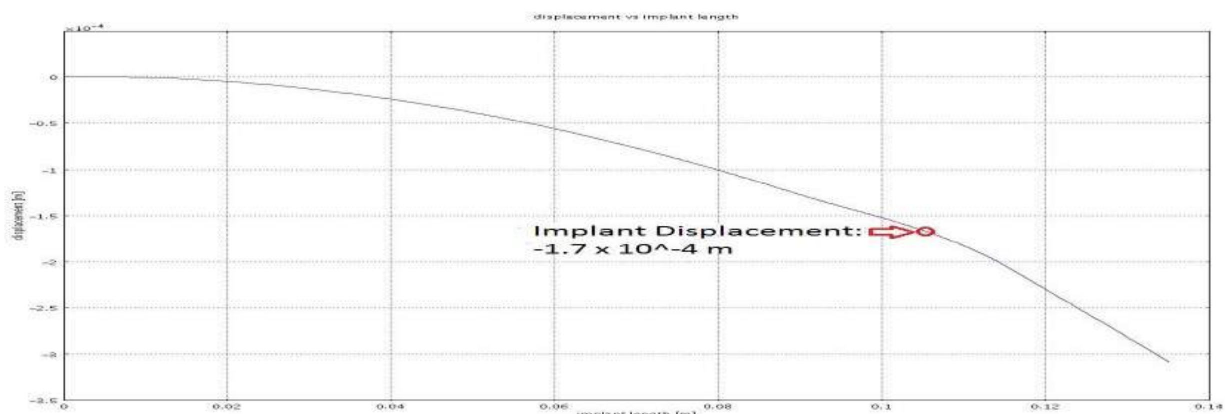

Figure 2 Displacement vs implant length curve generated by COMSOL. The implant displacement is indicated above. Displacement is roughly -1.7 x 10-4 m for the implant region between the first and second screw

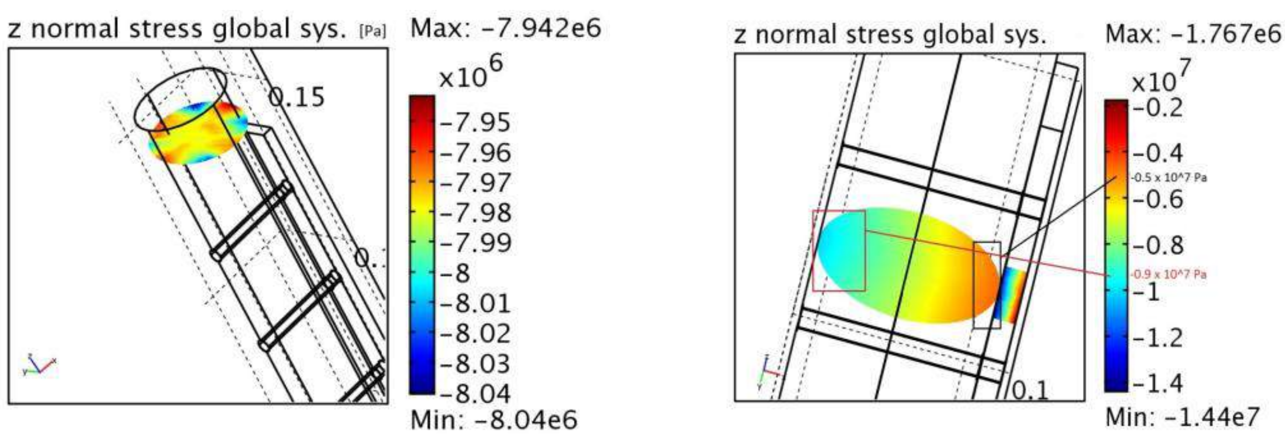

A) B)

Figure 3 .Normal stress distribution generated from COMSOL. A) A cross-sectional slice of the top of the bone unsupported by the implant reveals a stress of roughly -0.8 x 107 Pa . B) the bone region closest to the implant experiences a reduced stress of -0.5 x 107 Pa compared to the -0.9 x 107 Pa experienced by the region of bone farthest away from the implant.

Methods:

Our region of interest is the distal tibia, so we decided to model the portion of the tibia and the locking plate implant from just above the top of the implant to just above the ankle. For our geometric simplifications, we decided to follow an analytical model similar to the one found in S.-H. Kim et al (8). Using this model, we could approximate the tibia as a solid column, the implant plate as a rectangular plate, and the screws of the implant as solid cylinders which are made of the same material as the locking implant plate. We assumed that all materials were linear, elastic, homogeneous and isotropic. We felt that these assumptions were valid because the deformations in our bone, implant plate and screws should be small, given that the load we would apply to the bone was within physiologically relevant conditions according to an article by Wehner et al (5). From an article by Hobatho et al., we found that the tibia had an average Young's modulus of 10 GPa, a Poisson's ratio of 0.30, and a density of 1600 kg/m^3 (6). For our metal, we decided to use a TNTZ titanium alloy as reported in an article by Antonialli and Bolfarini (2). The article reported Young's modulus value of 50 GPa and a Poisson's ration of 0.34. We felt it was appropriate to use TNTZ as the metal for our implant and screws because TNTZ is a low-stiffness titanium alloy which is specifically designed for biomedical implants. We could not find an article which reported the density of TNTZ alloy, so we estimated it to be 4400 kg/m^3, which is around the values reported for lighter-weight titanium alloys (10). We set the diameter of our tibia to be 24.4 mm based upon a research article by Giladi et al. (7), and we found the dimensions of our implant from a distal tibia locking plate system designed by DePuy (4). A diagram of our model can be seen on Figure 4.

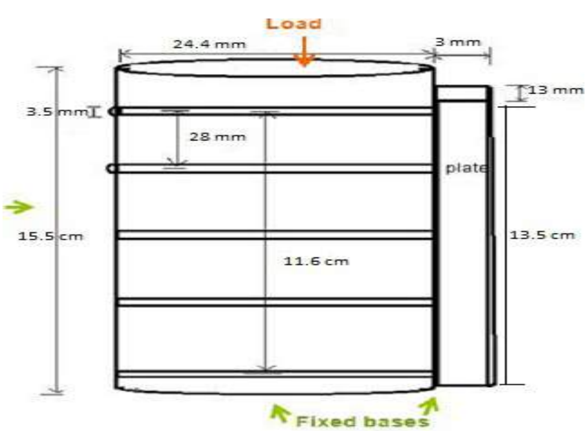

Figure 4: Model of distal tibia(indicated by the bigger cylinder) and locking plate(indicating by vertical rectangle and small horizontal cylinder)

For our boundary conditions, we followed similar conditions used by S.-H. Kim et al. by fixing the bottom end of the plate and the tibia and applying a constant axisymmetric downward axial load over the top surface of the tibia (8). We decided that these boundary conditions were appropriate because they are commonly used in biomechanical research articles which study implant plates and bone fractures. Similar to S.-H. Kim, we did not apply torsion. An article by Wehner, T. et al. revealed that internal loads in the human tibia during normal gait could produce a maximum force of up to 4.7 times a person's body weight (5). We decided to use this as our loading force to help us understand how the implant and bone behaved under the most intense loading situations experienced physiologically. We decided to calculate our loading force based off of an 80 kg person, which produced a loading force of 3688.56 N downward. This force was distributed over the top surface of the tibia with area of 4.62 x 10^{-4} m^2, resulting in a loading pressure of 7.98 x 10^6 Pa.

For our analytical model, we used a free body diagram of the whole implant region without the bone as indicated in Figure 4. From our preliminary COMSOL modeling, we found that most of the stress from loading concentrates on the first the screw. Also, only the part of plate between first screw and second screw experiences significant deflection, which we used as an estimate for potential displacement of the implant. Thus, our calculation for plate stress and deflection focused on the deflection of the part of plate between first screw and second screw. We assumed that the loading is evenly distributed in bone, so according to Figure 5, the solution for loading on screws (F_s) is:

$$F_s = \frac{F_{total}\,A_s}{A_b} = \frac{F_{total}\,dL}{\pi r^2}$$

A_s: Cross sectional area of screw
A_b: Total tibia cross sectional area
F_{total}: Total applied loading force
D: Screw diameter
L: Screw length (equal to tibia diameter)
(refer to figure 5 for parameter indication)

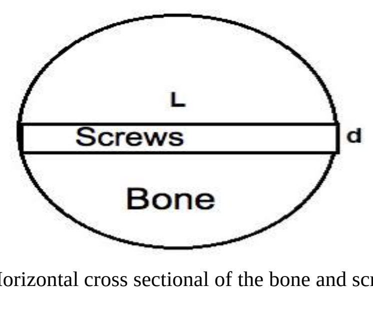

Figure 5. Horizontal cross sectional of the bone and screws.

After getting the F_s in Figure 5, we assumed this load is evenly distributed on each screw. This was the only way we could find loading on a single screw although the COMSOL modeling showed that the distribution of loading on the screws is uneven. Thus, the loading on first screw becomes $\frac{F_S}{N}$, where N stands for the number of screws. In our modeling scenario, we use 5 screws, but the actual number of screws in a single implant varies from case to case. The free body diagram for the implant is showed in Figure 6.

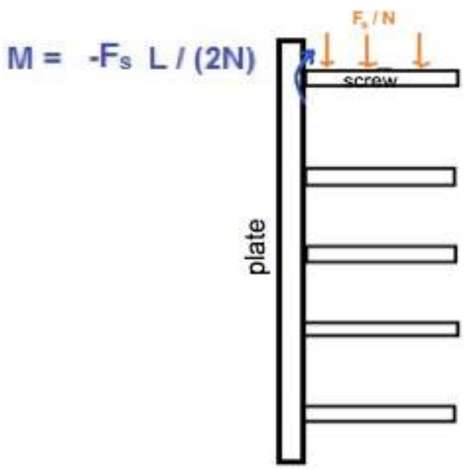

Figure 6. Free body diagram of the whole implant(the plate and screws)

We used the loading on the first screw to calculate the moment that the first screw applies on the plate. In this step, the plate end of the screw is assumed to be fixed. This assumption is reasonable because according to the COMSOL modeling based on 80kg body weight, the deflection will be really small. Figure 7 is a free body diagram for the first screw, which is taken to be a fixed-end beam with an evenly distributed load.

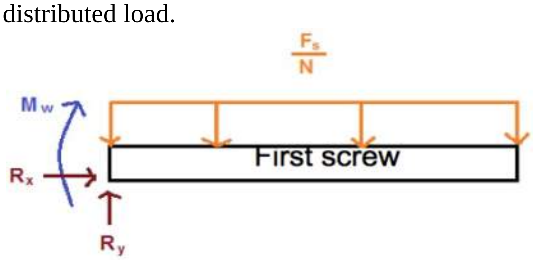

Figure 7. The free body diagram of the first screw only.

We used the method from Example 5.2 of our textbook to solve for the fixed end moment M_w in Figure 7 (12). We set F_S/N equal to the total force on the whole beam, making it equivalent to q_0L where L is the length of the screw.

$$\frac{F_s}{N} = q_oL$$

Thus, we use $\frac{F_S}{NL}$ in the calculation to replace q_0 and solve for M_w.

$$M_w = \frac{-F_sL}{2N}$$

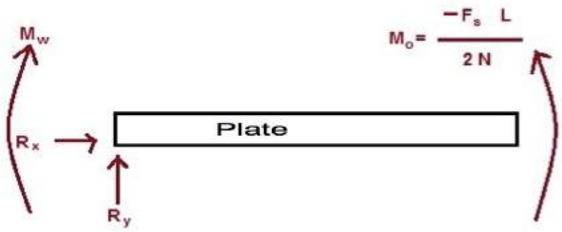

Figure 8. The free body diagram of the part of the plate between the first screw and the second screw. The first screw on the right is applied moment, the second screw on the left is fixed end. Mo is the applied moment.

After getting the moment in Figure 7, we solved for the moment in the portion of the plate between the first and second screws. The second screw end is assumed to be fixed such that the part of plate between first screw and second screw could be simplified to a beam with a fixed end and a pure moment applied at the free end, as shown in Figure 8. The reason for this assumption is that according to COMSOL modeling, even though the stress concentrates on first screw, the deflection of plate on the first screw end is very small. The deflection of the plate on the second screw end is even smaller, which allows us to neglect movement of the second screw and approximate it as a fixed end.

We used the method in example 5.6 in the textbook (12) to find the plate's internal moment

$$M_z = \frac{-F_sL}{2N}$$

We used equation 5.23 $\sigma_{xx} = -\frac{M_Z y}{I_{zz}}$ and equation 5.43 $EI_{zz}\frac{d^2\vartheta}{dx^2} = M_z(x)$. (12) to get stress and deflection on the portion of the plate between the first and second screw.

$$\sigma_{xx} = -\frac{M_z y}{I_{zz}} = \frac{3FdL^2}{\pi r^2 NbIr^2}$$

$$\vartheta = -\frac{3}{Ebh^3}\frac{Fx^2dL^2}{\pi r^2 N}$$

For the bone supported by the implant, we realized that the distribution of stress would be uneven due to the placement of the implant, and we did not know how to calculate an exact solution for the distribution of stress. However, we expected the stress to be lowest in the portion of the bone closest to the implant plate; we thought that the bone close to the implant should be supported by the implant, reducing the stress in the bone.

Discussion:

Comparing the results from our analytical model and our COMSOL model, we saw that our calculations for stress and displacement were within the same order of magnitude as the COMSOL calculations. This implies that our calculations could provide a good first approximation of stress and deflection. We saw that there was a 95.8% difference between the stress values and a 43.9% difference in the deflection values. A possible reason for the difference in stress could be that we had not properly included all forces at the plate-screw interface, which would explain why our stress value was so much lower than COMSOL's value. An explanation for the differences in displacement / deflection values could be that we had fixed the ends of our screws inside the implant when, in reality, the screw ends are not actually fixed. Freedom of movement at the first and second screw end positions could allow for a reduction of applied moment to the implant, reducing the amount of deflection or displacement in the implant.

We believe that the significant stress concentration around the first and second screw positions (Fig. 1A) could provide a possible explanation for patient complaints about pain. An article by Gille et al. indicate that screw perforations and patient pain are two complications which can lead to plate removal. We believe that there may be a link between the high stress around the first and second screw positions and patient pain. Perhaps the concentration of stress around the screws leads to bruising of the tissue and bone, resulting in patient discomfort.

From a comparison of the bone stress in Figure 3A and Figure 3B, we saw that there was a 37.5% decrease in stress near the implant compared to the bone unsupported by the implant; this was within expectations. However, we did not expect the increase in stress from -0.8×10^7 to -0.9×10^7 Pa. A possible reason for this increase in stress near the edges of the bone may be that downward displacement of the screw causes an increase in stress in the surrounding bone. We believe that this uneven stress distribution in the tibia bone may lead to uneven bone density in the tibia, with low bone density located close to the implant and high bone density located near the edge of the bone opposite to the implant.

We also considered the accuracy of our COMSOL model. Based upon an article by Wieding et al demonstrated that modeling screws as solid cylinders could potentially lead to inaccurate modeling of stress in the bone (11). Also, we only modeled a portion of the tibia. In the future, we could refine the model of the screws of our implant to include threading, and we could also try to model the whole tibia bone. We could also try to model our bone as an anisotropic material, as was done by S.-H. et al (8).

Conclusion:

Our group found that clinical observations about patient reactions to implants and implant complications could potentially be explained by finite element analysis. Patient discomfort from implants could be the result of high stress concentration around anchoring points like the screws in our tibia model. Potential areas of bone density loss and density gain could also be predicted by looking at the distribution of stress in a finite element model. We believe that researchers could try to apply finite element analysis to describe mechanical reasons behind clinical observations.

References:

1. *Materials Science Graduate Programs – Bone implant research leaps forward.* Washington State University. < http://www.wsu.edu/materials/bone-implant.html>. Accessed 5 Dec. 2012.
2. Antonialli A, Bolfarini C (2011) Numerical Evaluation of Reduction of Stress Shielding in Laser Coated Hip Prostheses. *Materials Research* 14(3): 331-334.
3. Gille J, et al. (2012) Arthroscopic-assisted removal of proximal tibia locking plates. *Sports Medicine, Arthroscopy, Rehabilitation, Therapy & Technology* 4(18): 1-5.
4. (2010) ALPS Distal Tibia Plate System – Anterolateral & Medial Distal Tibia Locking Plates, Surgical Technique. Manual distributed DePuy, a Johnson & Johnson company.
5. Wehner T, Claes L, Simon U (2009) Internal loads in human tibia during gait. *Clinical Biomechanics* 24: 299-302.
6. Hobatho MC, Darmana R, Barrau JJ, Laroze S, Morucci JP (1988) Relationship Between Mechanical Properties of the Tibia and its Natural Frequencies. *IEEE Engineering in Medicine & Biology Society 10th Annual International Conference*: 681-682.
7. Giladi M, et al. (1987) Stress Fractures and Tibial Bone Width. The *Journal of Bone and Joint Surgery* 69(2): 326-329.
8. Kim S-H, Chang S-H, Jung H-J (2010) The Finite Element Analysis of a fractured tibia applied by composite bone plates considering contact conditions and time-varying properties of curing tissues. *Composite Structures* 92: 2109-2118.
9. Latifi MH, et al. (2012) Prospects of implant with locking plate in fixation of subtrochanteric fracture: experimental demonstration of its potential benefits on synthetic femur model with supportive hierarchical nonlinear hyperelastic finite element analysis. *BioMedical Engineering OnLine* 11(23): 1-18.
10. *Titanium Alloys – Physical*. The A to Z of Materials – AZOM.com, 2 Apr. 2002. <http://www.azom.com/article.aspx?ArticleID=1341>. Accessed 7 Nov. 2012.
11. Wieding J, Souffrant R, Fritsche A, Mittelmeier W, Bader R (2012) Finite Element Analysis of Osteosynthesis Screw Fixation in the Bone Stock: An Appropriate Method for Automatic Screw Modelling. *PLoS ONE* 7(3): e33776. doi:10.1371/journal.pone.0033776.
12. Humphrey JD, DeLange SL. *An Introduction to Biomechanics: Solids and Fluids, Analysis and Design*. New York: Springer-Verlag, 2004.